JTTEE5 5:463-468

The Application of Thermal Sprayed Coatings for Pig Iron Ingot Molds

H.-J. Kim and Y.-G. Kweon

Molds made of gray cast iron for casting pig iron ingots are subjected to severe temperature fluctuations. The main life-limiting factor for mold damage is the formation of surface cracks arising from thermal fatigue. Various flame and plasma sprayed coatings were investigated to extend the life of these molds. Coating materials studied include plasma sprayed ceramic coatings with bond coats as well as flame sprayed oxidation-resistant alloy powders.

The results of cyclic furnace tests from room temperature to 1100 °C in air, simulating the thermal cycle in casting, indicated that failure occurred along the interface between the bond coat and the gray iron substrate because of iron oxidation, and not at the interface between the ceramic top coating and the bond coating for a superalloy substrate. The field test results indicated that plasma sprayed alumina coatings with 200 μm top coating thickness are the most promising materials for pig iron casting.

Keywords alumina coatings, pig iron molds, protective coatings, thermal cycling

1. Introduction

MOLDS made of gray cast iron for casting pig iron ingots are subjected to severe temperature fluctuations in a manner similar to those in the die casting process except that the principal damage mechanism is high pressure erosion caused by the molten metal. Therefore, the main life-limiting factor for mold damage is surface cracking arising from thermal fatigue. Recently, work on the thermal fracture endurance of pig iron ingot molds manufactured from flake, compacted graphite, and spheroidal graphite cast irons was reported (Ref 1), and concluded that compacted graphite cast iron exhibited a better thermal fracture endurance than flake or spheroidal graphite cast irons.

The purpose of our investigation was to improve the thermal fatigue properties of gray cast iron for molds by modifying the surface to improve the detachability of solidified pig iron from the mold and thus extend the life of the mold. Various flame and plasma sprayed coatings were studied for mold coatings suited for a range of mold sizes and materials, operating temperatures, and costs.

Few reports on the application of the thermal spraying technique to melting operations have been published. However, compared to pig iron casting temperatures, the temperatures of these operations are lower for nonferrous alloys (Ref 2, 3) or higher for refractory metals (Ref 4-6). Flame sprayed coatings for slag holes in blast furnaces and for refractory linings are reported in Ref 7 and 8. However, these applications are dissimilar to the present one because these molds are both lubricated and water cooled.

H.-J. Kim and **Y.-G. Kweon,** Research Institute of Industrial Science and Technology, Maintenance Technology Research Team, P.O. Box 135, Pohang, 790-600, Korea.

2. Experimental Methods

2.1 *Coating Method*

Metco 5P-II and Sulzer F4 (PT-M1100) equipment (Sulzer Metco, Westbury, NY) was used for flame and plasma spraying, respectively. The substrate was a gray cast iron (FC20) used for mold materials. The coating thickness was approximately 300 μm; cross-sectional microstructures are shown in Fig. 1. All the coatings were supplied by a commercial thermal spraying job shop using their recommended process parameters.

2.2 *Simulated Cyclic Furnace Tests*

Preliminary thermal cycling tests in air were conducted as shown in Fig. 2. Room temperature tap water was sprayed for 2 to 3 s onto the coating to wet the surface just before each heating cycle. The specimen was 100 by 50 by 5 mm thick. The onset of cracking and estimated time for 20% spallation from the coating surface were observed by the eye.

2.3 *Field Test Evaluation*

Based on the results of the cycling tests, coatings were selected for field testing. First, 12 coated 100 by 50 by 5 mm specimens were prepared in a mold for a field test. However, the test was interrupted after approximately 140 cycles due to excessive attachment of solidified pig iron to the tested mold surface.

The next approach was to coat the whole surface of each mold with a single coating. Coating materials tested in this trial are listed in Table 1. The molds experienced the following thermal cycle: heating by molten iron at 1450 °C, air cooling for 80 s to allow for the solidification of the molten iron, water spraying for 120 s to enhance cooling, shaking out the pig iron, and air cooling of the empty molds for about 240 s before the second round of pouring. These molds were sprayed for 20 s with a mixture of graphite, slaked lime, and water during the air cooling of the empty molds to prevent the mold surface from directly contacting molten iron on the subsequent iron pouring step. This spray procedure reduces the severity of thermal shock.

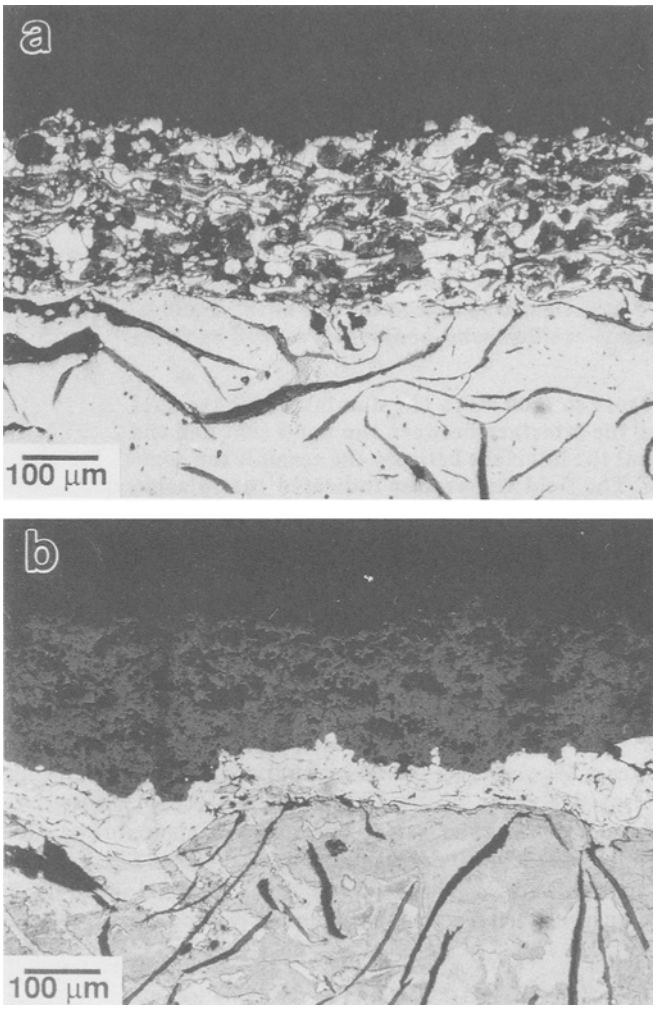

Fig. 1 Typical cross-sectional microstructures of coated specimens. (a) One-layered coating (flame spray) and (b) two-layered coating (plasma spray)

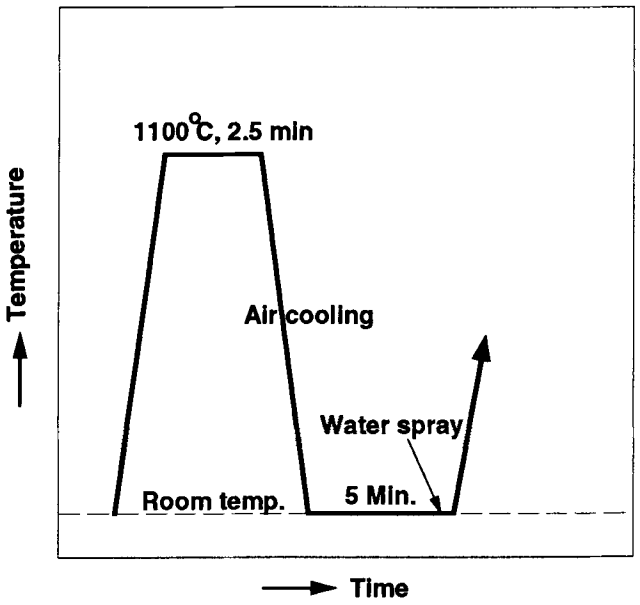

Fig. 2 Schematic representation of the thermal fatigue testing cycle in air

Table 1 Description of field tested specimens

Specimen No.	Description
0	Uncoated mold (gray cast iron)
1	NiCrAl (Metco 443NS) 100 μm + ZrO_2-24MgO (Metco 210) 200 μm
2	NiCrAl (Metco 443NS) 100 μm + ZrO_2-8Y_2O_3 (Amdry* 6610) 200 μm
3	NiCrAl (Metco 443NS) 100 μm + Al_2O_3 (Metco 105) 200 μm
4	NiCrAl (Metco 443NS) 100 μm + ZrO_2-8Y_2O_3 (Metco 204) 300 μm
5	NiCrAlY (Amdry 961) 100 μm + ZrO_2-8Y_2O_3 (Metco 204) 200 μm
6	NiCrAlCoY (Metco 461NS) 100 μm + ZrO_2-8Y_2O_3 (Metco 204) 200 μm
7	NiCrAl (Metco 443NS) 100 μm + 25%Al_2O_3: 75%Ni5Al (Amdry 956) 100 μm + Al_2O_3 (Metco 105) 100 μm
8	NiCrAl (Metco 443NS) 100 μm + 75%Al_2O_3: 25%Ni5Al (Amdry 956) 100 μm + Al_2O_3 (Metco 105) 100 μm
9	NiCrAl (Metco 443NS) 100 μm + 50%Al_2O_3: 50%Ni5Al (Amdry 956) 100 μm + Al_2O_3 (Metco 105) 100 μm

*Amdry (Sulzer Surface Technology Company, Plasma-Technik AG, CH-5610 Wohlen, Switzerland)

Evaluation of the performance of each coating was carried out by measuring the total number of cracks (n), the maximum crack length (D_{max}), the average crack length (D_{ave}), the total crack length (T), and the total crack area ($n \times D_{ave}^2$) in a mold. A typical crack pattern in a mold is shown in Fig. 3. Note that most of the main cracks for both coated and uncoated molds were parallel to the direction of molten iron flow, which is perpendicular to the longer dimension of the rectangular molds in Fig. 3. An expected benefit of a ceramic coating was that solidified pig iron would shake out better from ceramic coated molds than from uncoated molds even if the coated molds exhibited the same crack length and density.

3. Results and Discussion

3.1 *Simulated Cyclic Furnace Tests*

The results of cyclic furnace tests in air are shown in Fig. 4. The failure of the plasma sprayed ZrO_2-24MgO coating (B) and the powder flame-sprayed NiCr coating (D) was by cross-sectional fracture of the whole specimen rather than spalling of the coating. The spalling of the coating started around the center of the specimen. The poor performance of the flame-sprayed alumina and alumina/titania coatings are considered to be due to their high proportion of unmelted particles and high porosity.

The cross-sectional view (backscattered electron) of the NiCr coating after the thermal cycling test is shown in Fig. 5. The No. 1 region is NiO and $NiCr_2O_4$, as determined by energy-

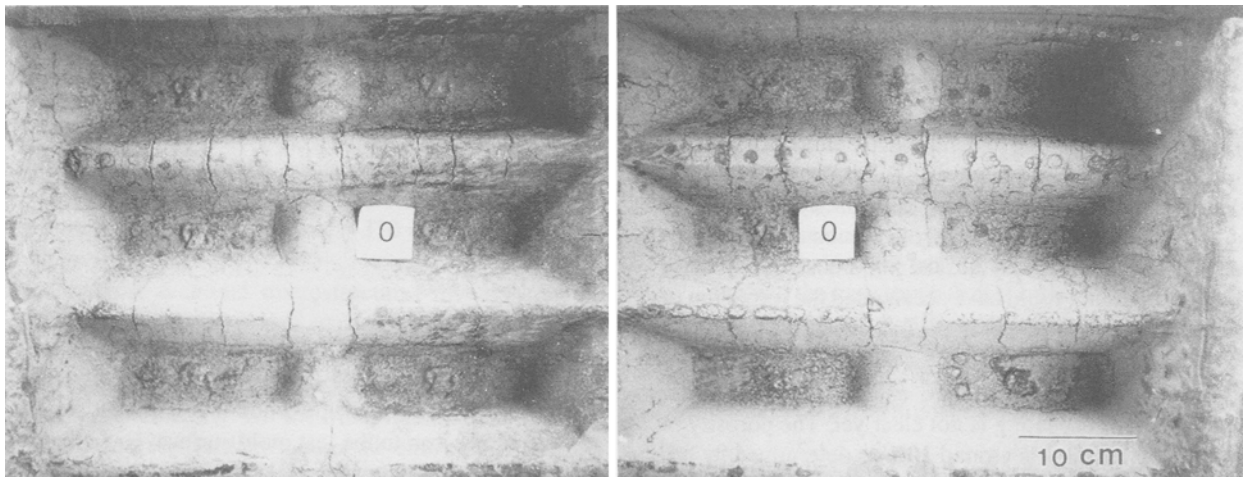

Fig. 3 Typical surface morphology of field tested mold specimen showing many vertical cracks

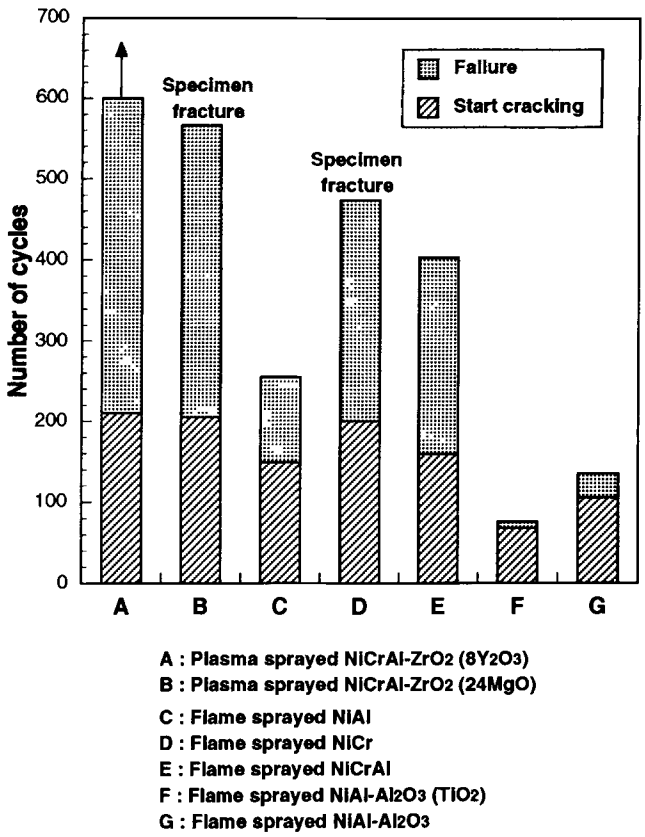

Fig. 4 Results of thermal cycling tests in air

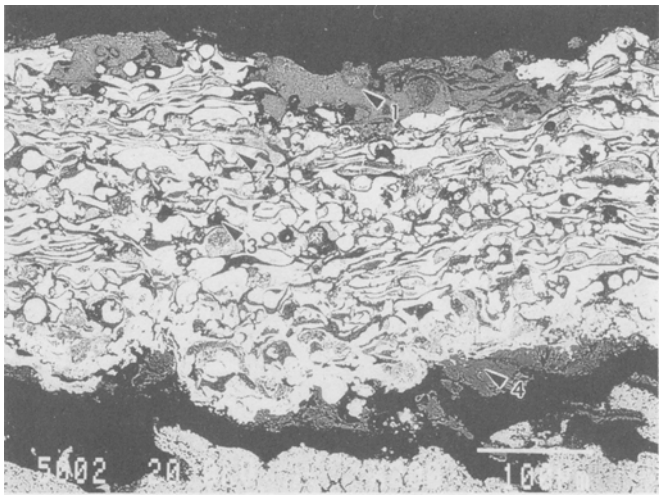

Fig. 5 Backscattered electron image of flame sprayed NiCr coating after thermal cycling test in air

Table 2 EDS analysis of flame sprayed NiCr coating after thermal cycling test in air from Fig. 5

	Composition, wt.%			
Position No.	Ni	Cr	Fe	Si
1	96.4	3.6	...	...
2	91.9	8.1	...	...
3	10.3	87.2	...	2.5
4	...	0.5	99.5	...

dispersive spectroscopy (EDS) analysis (Table 2) and x-ray diffraction (XRD). The No. 4 region is considered to be iron oxide based on Table 2. The failure clearly occurred along the iron oxide layer between the bond coating and the gray iron substrate. Spalling of the NiAl and NiCrAl coatings also occurred along an iron oxide layer between the bond coating and the gray iron substrate.

A backscattered electron image of the ZrO_2-24MgO coating after thermal cycling is shown in Fig. 6 where a thick iron oxide layer formed between the bond coat and the gray iron substrate. Many vertical cracks exist in the ceramic top coating, but one large crack, as indicated by the arrow, propagates through the iron oxide layer and the substrate although blunting of the crack seems to have occurred in the bond coating.

On the other hand, the ZrO_2-$8Y_2O_3$ coating after the thermal cycling test has no sign of iron oxide formation under its bond coat, as shown in Fig. 7. The only difference before and after the thermal cycling test is the existence of the vertical cracks. The

vertical cracks stop at the bond coating and propagate along the ceramic coating as indicated by the arrow in region B.

It has been reported that the failure of thermal barrier coatings occurs mostly along the interface between the ceramic top coating and the bond coat due to bond coat oxidation for a superalloy substrate (Ref 9-12). However, failure for the gray iron substrate in the present case occurred along the iron oxide layer between the bond coating and the gray iron substrate, not at the interface between the top coat and the bond coat. Spraying of water during the testing could have accelerated the formation of the iron oxide layer because the water could penetrate to the substrate through the pores of the coating.

The reason why the ZrO_2-$8Y_2O_3$ coating performs better than the ZrO_2-24MgO coating is not clear yet. The porosity of both ceramic top coatings is around 10% as determined by image analysis. Furthermore, tetragonal to monoclinic phase transformation after the thermal cycling test was measured to be negligible (Ref 13). This result is consistent with the test reports in air (Ref 14, 15). That is, the tetragonal to monoclinic phase transformation is only noticeable at 1400 °C or above. Obviously, water spraying on the coating surface during the thermal cycling test did not cause the phase transformation of zirconia-based coatings as reported by Yasuda et al. (Ref 16) and Sato and Shimada (Ref 17).

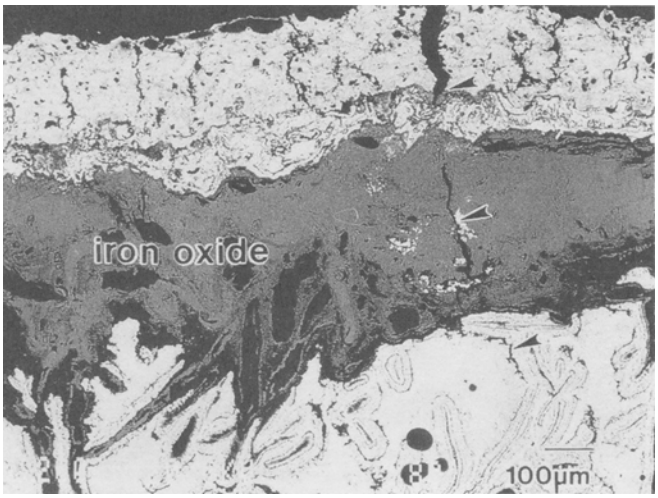

Fig. 6 Backscattered electron image of plasma sprayed ZrO_2-24MgO coating after thermal cycling test in air

3.2 *Field Tests*

Based on the thermal cycling tests in air, 12 coating specimens mounted in a mold were tested in a pig iron production line. This test was interrupted due to significant attachment of solidified pig iron to the test mold surface. Examination of the coating microstructures revealed comingling of the metallic coatings and the solidified iron. Erosion of the ceramic top coating occurred as shown in Fig. 8. Therefore, powder flame-sprayed metallic coatings were excluded from further field tests because the erosion behavior led to attachment of the metallic coating and the solidified iron. Plasma sprayed alumina coatings were tested further because of their excellent wear resistance and better properties.

For the whole-mold coatings, the variations of maximum crack length and total crack area as a function of operating cycle are shown in Fig. 9 and 10, respectively. The crack dimension was measured without grinding the surface; thus the values sometimes appeared to decrease as the test proceeded. This can be explained by the fact that solidified iron can penetrate the cracks during the cycle making the measurements misleading. Another explanation is that cracking propagated along a main crack after the formation of the first few cracks, and the thermal stress was then dissipated in extending the main cracks instead of creating more new cracks. These phenomena are typical for flake cast iron as reported in Ref 1 and were confirmed by the cross-sectional examination (both parallel and perpendicular to the main cracks) of 5,000 cycled molds. Therefore, the thermal fatigue cracking behavior of fully

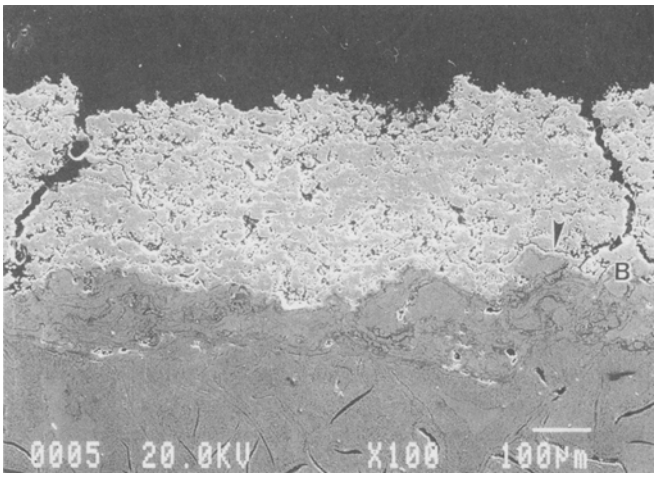

Fig. 7 Cross-sectional scanning electron microscopy (SEM) image of plasma sprayed ZrO_2-$8Y_2O_3$ coating after thermal cycling test in air

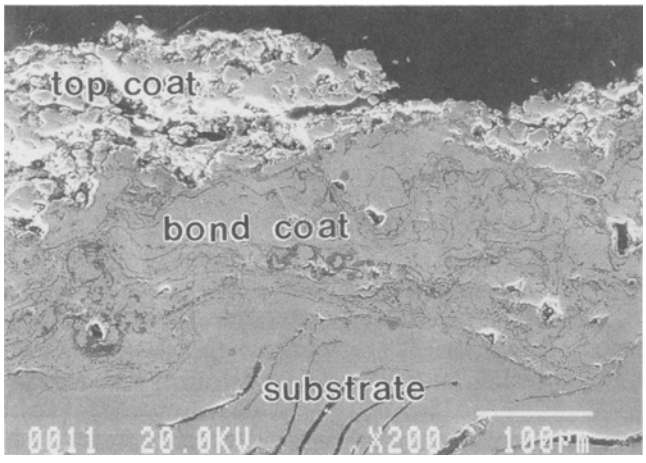

Fig. 8 Cross-sectional microstructure of ZrO_2-$8Y_2O_3$ coating after approximately 140 operating cycles exposed to iron casting environments

coated gray iron molds is expected to be very similar to that of uncoated gray iron molds.

Mold life is evidently governed mostly by maximum crack length, and the detachability of solidified pig iron from molds is governed mostly by total crack area. Plasma sprayed alumina-based and ZrO_2-$8Y_2O_3$ based coatings with 200 μm top coating thickness are the most promising materials after approximately 5,000 operating cycles (approximately 110 operating days) as shown in Fig. 9 and 10.

However, cross-sectional microstructural investigation of 5,000 cycled molds revealed that erosion of the coatings was caused by molten iron as indicated in Fig. 11. Most ZrO_2-24MgO coatings were eroded, and an iron oxide layer was attached to the bond coating. On the other hand, about 100 μm thick alumina coatings remained over the entire bond coating surface. The coated molds behaved better than the uncoated ones until around 3,000 cycles, and then their performance fell down (Fig. 9 and 10) because of either erosion or spalling of the ceramic top coatings in service. Note that both bond coatings in Fig. 11 are virtually intact even after approximately 5,000 operating cycles. Therefore, mold life and detachability of the solidified pig iron from molds were independent of the bond coating materials used. Thus, plasma sprayed alumina coatings with 200 μm top coating thickness were the most promising materials for pig iron casting environments taking also into account cost and erosion resistance.

4. Conclusions

- The results of simulated thermal cycling tests from room temperature to 1100 °C in air indicated that coating failure occurred along the iron oxide layer between the bond coating and the gray iron substrate, not at the interface between the ceramic top coating and the bond coating.
- Erosion of coating materials by molten iron was observed in actual pig iron ingot production cycles.
- Most of the bond coatings remained virtually intact after approximately 5,000 operating cycles (approximately 110 operating days). Therefore, mold life and detachability of the solidified pig iron from molds were independent of the bond coating materials used.
- Plasma sprayed alumina coatings with 200 μm top coating thickness were the most promising materials for pig iron casting environments taking into account cost and erosion resistance.

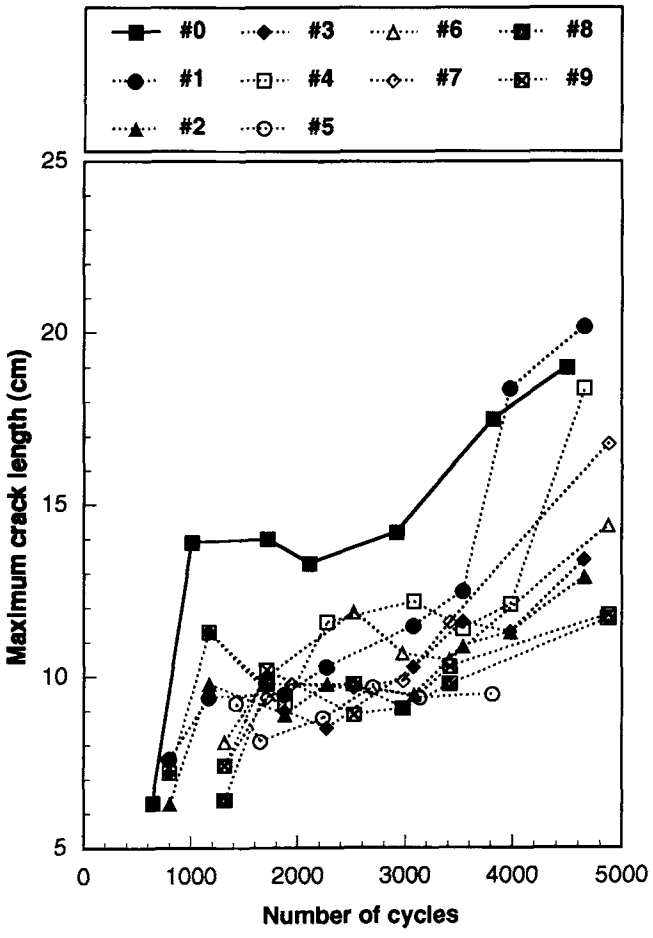

Fig. 9 Maximum crack length in a mold as a function of operating cycles. Sample codes are given in Table 1.

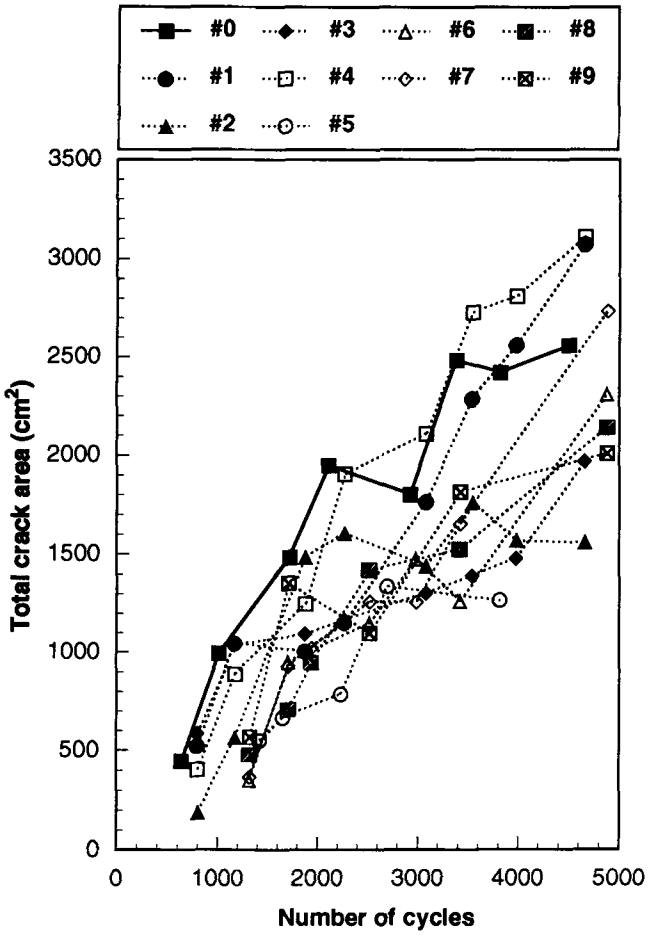

Fig. 10 Total crack area in a mold as a function of operating cycles. Sample codes are given in Table 1.

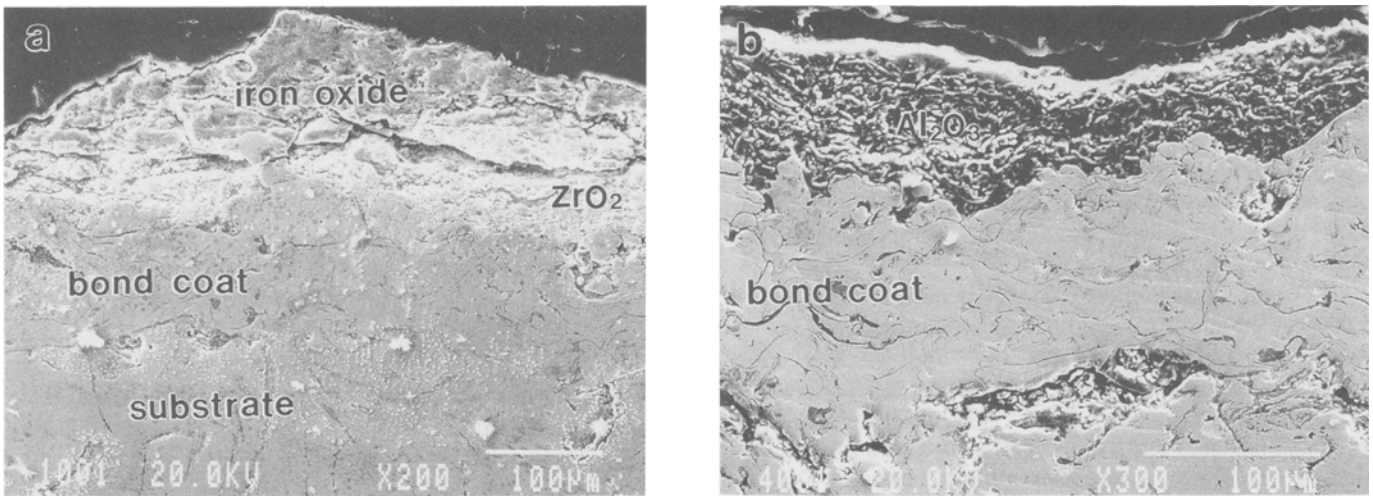

Fig. 11 Cross-sectional microstructures of plasma sprayed coatings on cast iron molds after approximately 5,000 operating cycles for pig iron ingot production. (a) ZrO_2-24MgO and (b) Al_2O_3

References

1. J.L. Lee and S.C. Lee, Thermal Fracture Endurance of Cast Irons with Application Study of Pig Iron Ingot Molds, *Metall. Trans. A,* Vol 26, 1995, p 1431-1440
2. Y. Shimizu, M. Sato, M. Kobayashi, and T. Ikeda, Applicability of Thermally Sprayed Zirconia Coatings to Casting Mold Dressings, *Thermal Spray Research and Application,* T.F. Bernecki, Ed., ASM International, 1990, p 521-526
3. M.D. Modi, S.C. Modi, and M.M. Mayuran, A Case Study on the Use of Plasma Sprayed Oxide Ceramic Coatings in Hot Extrusion Dies for Non-Ferrous Metals, *Advances in Thermal Spraying,* 8-12 Sept 1986, Welding Institute of Canada, p 359-366
4. D.J. Sordelet, T.W. Ellis, and I.E. Anderson, Non-Contaminating Plasma Arc Sprayed Crucible Coatings for Containing Molten Ceramic Oxides, *J. Therm. Spray Technol.,* Vol 2, 1993, p 385-392
5. E.L. Bird and C.E. Holcombe, Jr., Investigation of Plasma Sprayed Laminates for High Temperature Melting Operations, *Thermal Spray: International Advances in Coatings Technology,* C.C. Berndt, Ed., ASM International, 1992, p 625-629
6. T.W. Ellis, D.L. Sordelet, and F.C. Laabs, Evaluation of Plasma Sprayed Crucible Coatings for Melt Processing Copper-Refractory Metal Alloys, *Thermal Spray: International Advances in Coatings Technology,* C.C. Berndt, Ed., ASM International, 1992, p 631-636
7. G. Jiacheng and Z. Yaping, Application of Graded Ceramic Coatings for Thermal Barriers, *Surf. Coat. Technol.,* Vol 63, 1994, p 93-96
8. H. Grutzner and H. Weiss, Development of Plasma Sprayed Ceramic Coatings against Slag Attack for the Steel Industry, *Advances in Thermal Spraying,* 8-12 Sept 1986, Welding Institute of Canada, p 349-358
9. B.C. Wu, E. Chang, S.F. Chang, and D. Tu, Degradation Mechanisms of ZrO_2-8 wt.% Y_2O_3/Ni-22Cr-10Al-1Y Thermal Barrier Coatings, *J. Am. Ceramic Soc.,* Vol 72 (No. 2), 1989, p 212-218
10. R.D. Maier, C.M. Scheuermann, and C. W. Andrews, Degradation of a Two Layer Thermal Barrier Coating under Thermal Cycling, *J. Am. Ceramic Soc.,* Vol 60 (No. 5), 1981, p 555-561
11. R.A. Miller and C.E. Lowell, Failure Mechanisms of Thermal Barrier Coatings Exposed to Elevated Temperatures, *Thin Solid Films,* Vol 119, 1984, p 173-184
12. R.A. Miller, Oxidation-Based Model for Thermal Barrier Coating Life, *J. Am. Ceramic Soc.,* Vol 67 (No. 8), 1984, p 517-521
13. RIST research project 94A126, Pohang, Korea, 1995
14. J.R. Brandon and R. Tayer, Phase Stability of Zirconia-Based Thermal Barrier Coatings. Part I. Zirconia-Yttria Alloys, *Surf. Coat. Technol.,* Vol 46, 1991, p 75-90
15. R.A. Miller, J.L. Smialek, and R.G. Garlick, Phase Stability in Plasma-Sprayed Partially Stabilized Zirconia-Yttria, *Science and Technology of Zirconia, Advances in Ceramics,* Vol 3, A.H. Heuer and L.W. Hobbs, Ed., The American Ceramic Society, 1981, p 241-253
16. K. Yasuda, S. Suenaga, K. Wada, S. Arai, M. Itoh, and H. Takeda, Phase Transformation of Plasma Sprayed Zirconia-Yttria Coatings during Hydrothermal Aging, *Thermal Spraying, Current Status and Future Trends,* A. Ohmori, Ed., High Temperature Society of Japan, 1995, p 1139-1144
17. T. Sato and M. Shimada, Transformation of Yttria-Doped Tetragonal ZrO_2 Polycrystals by Annealing in Water, *J. Am. Ceramic Soc.,* Vol 68 (No. 6), 1985, p 356-359